

# Cooperative Carbon Dioxide Capture in Diamine-Appended Magnesium–Olsalazine Frameworks

Ziting Zhu, Surya T. Parker, Alexander C. Forse, Jung-Hoon Lee, Rebecca L. Siegelman, Phillip J. Milner, Hsinhan Tsai, Mengshan Ye, Shuoyan Xiong, Maria V. Paley, Adam A. Uliana, Julia Oktawiec, Bhavish Dinakar, Stephanie A. Didas, Katie R. Meihaus, Jeffrey A. Reimer, Jeffrey B. Neaton, and Jeffrey R. Long\*

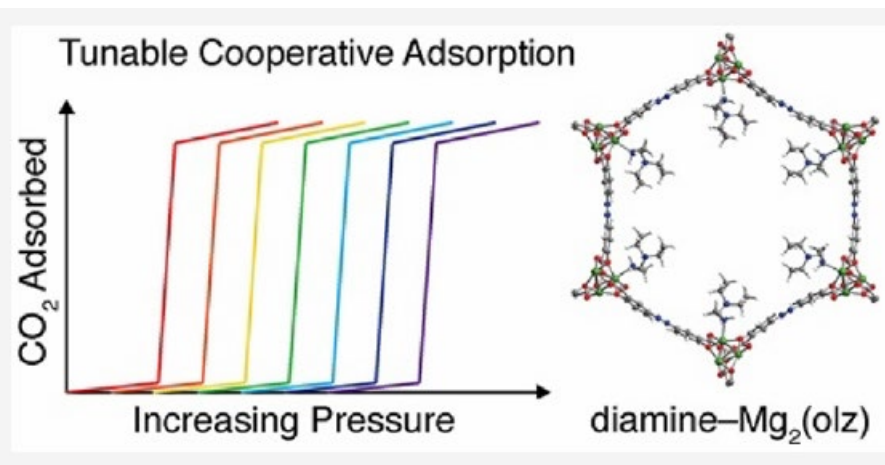


Cite This: *J. Am. Chem. Soc.* 2023, 145, 17151–17163



Read Online

Jeffrey R. Long– Department of Chemical and Biomolecular Engineering and Department of Chemistry, University of California, Berkeley, California 94720, United States; Materials Sciences Division, Lawrence Berkeley National Laboratory, Berkeley, California 94720, United States.



Sonali Seth  
04.05.2024

Published on July 26, 2023

# Background

## PERSPECTIVE

# Amine Scrubbing for CO<sub>2</sub> Capture

Gary T. Rochelle

Amine scrubbing has been used to separate carbon dioxide (CO<sub>2</sub>) from natural gas and hydrogen since 1930. It is a robust technology and is ready to be tested and used on a larger scale for CO<sub>2</sub> capture from coal-fired power plants. The minimum work requirement to separate CO<sub>2</sub> from coal-fired flue gas and compress CO<sub>2</sub> to 150 bar is 0.11 megawatt-hours per metric ton of CO<sub>2</sub>. Process and solvent improvements should reduce the energy consumption to 0.2 megawatt-hour per ton of CO<sub>2</sub>. Other advanced technologies will not provide energy-efficient or timely solutions to CO<sub>2</sub> emission from conventional coal-fired power plants.

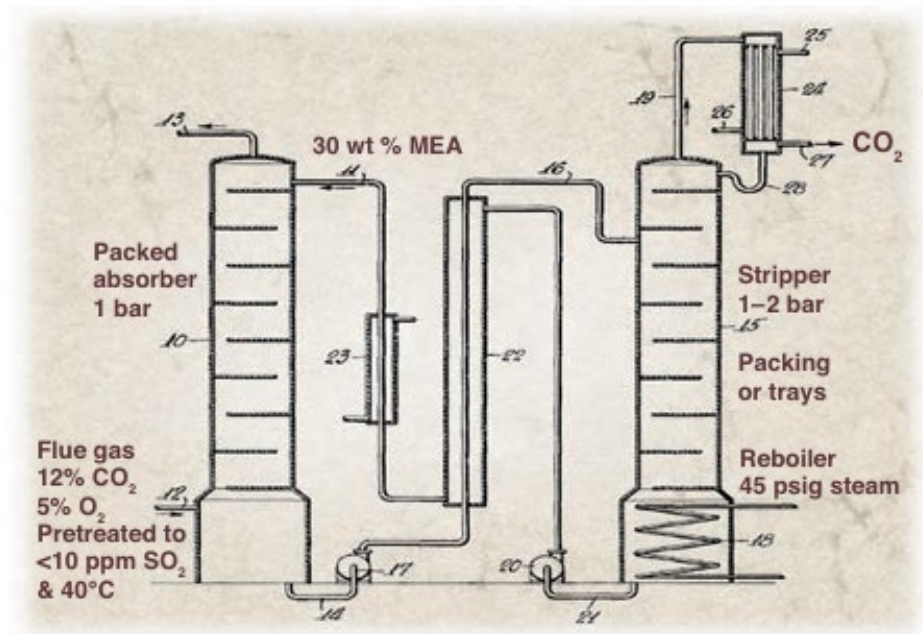


**Fig. 1.** The amine scrubbing process invented by Bottoms in 1930 (7).

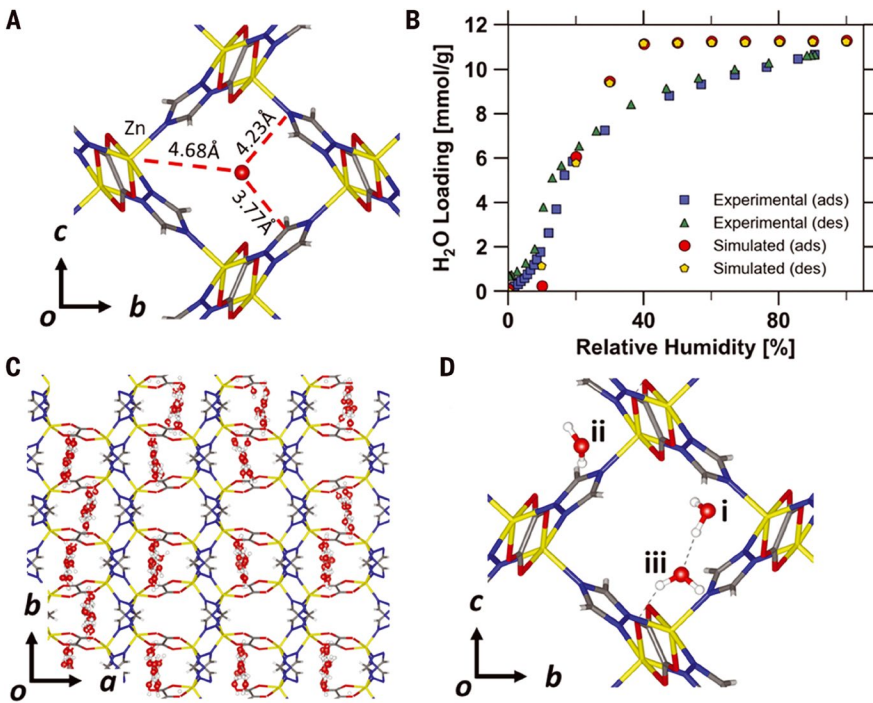
RESEARCH ARTICLE | CARBON CAPTURE

f X in

# A scalable metal-organic framework as a durable physisorbent for carbon dioxide capture

JIAN-BIN LIN, TAI T. T. NGUYEN, RAMANATHAN VAIDHYANATHAN, JAKE BURNER, JARED M. TAYLOR, HANA DUREKOVA, FARID AKHTAR, ROGER K. MAH, OMID GHAFARI-NIK, AND GEORGE K. H. SHIMIZU +8 authors Authors Info & Affiliations

SCIENCE • 16 Dec 2021 • Vol 374, Issue 6574 • pp. 1464-1469 • DOI:10.1126/science.abc7281

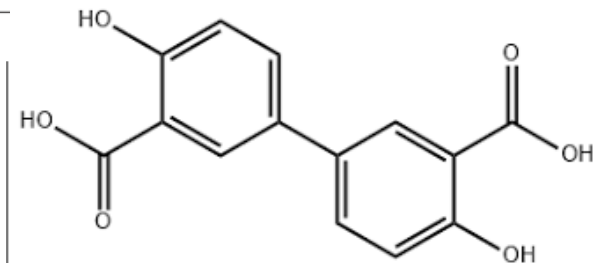


## RESEARCH ARTICLE

## GAS SEPARATIONS

## Cooperative carbon capture and steam regeneration with tetraamine-appended metal–organic frameworks

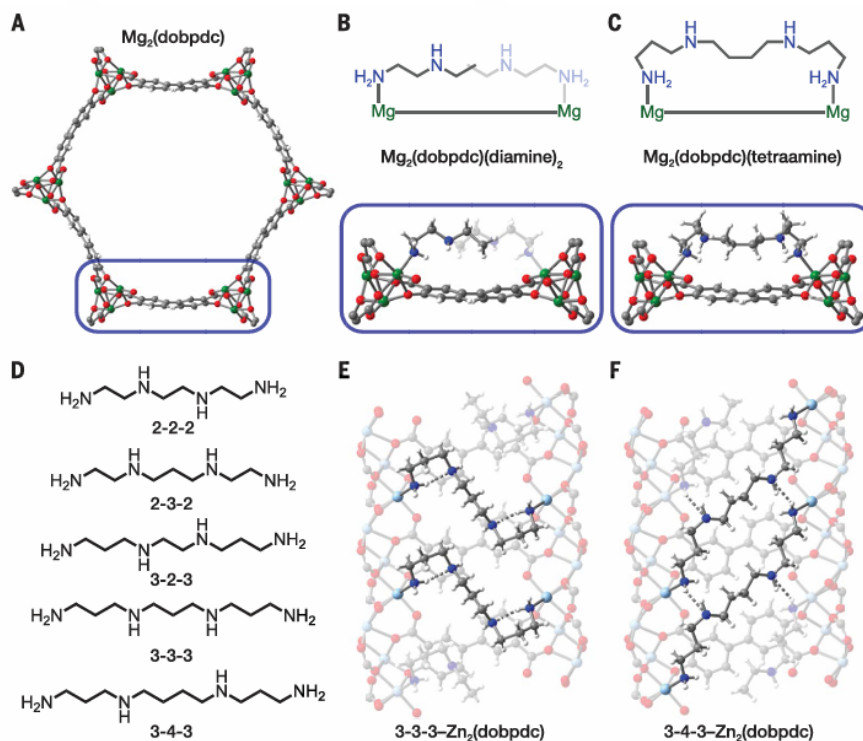
Eugene J. Kim<sup>1</sup>, Rebecca L. Siegelman<sup>1,2,\*</sup>, Henry Z. H. Jiang<sup>1</sup>, Alexander C. Forse<sup>1,3,4,†</sup>, Jung-Hoon Lee<sup>5,6,7</sup>, Jeffrey D. Martell<sup>1,†</sup>, Phillip J. Milner<sup>1,§</sup>, Joseph M. Falkowski<sup>8</sup>, Jeffrey B. Neaton<sup>5,6,9</sup>, Jeffrey A. Reimer<sup>2,3</sup>, Simon C. Weston<sup>8</sup>, Jeffrey R. Long<sup>1,2,3,¶</sup>



Cross-linker

(dobpdc4=4,4' dioxidobiphenyl-3,3'-dicarboxylate)

**Fig. 1. Diamine versus tetraamine coordination in  $M_2(\text{dobpdc})$ .** (A) Illustration of a hexagonal channel of  $\text{Mg}_2(\text{dobpdc})$  viewed in the  $ab$ -plane, using single-crystal XRD data for the isostructural framework  $\text{Zn}_2(\text{dobpdc})$ . (B and C) Diamine-functionalized material features coordination of one diamine to each  $\text{Mg}^{2+}$  site (28) (B), whereas tetraamines can coordinate to two  $\text{Mg}^{2+}$  sites (C). (D) Tetraamines explored in this work and their abbreviations. (E and F) Single-crystal XRD structures (100 K) of  $\text{Zn}_2(\text{dobpdc})$  functionalized with 3-3-3 and 3-4-3 tetraamines, respectively. The tetraamines span metal centers across the pore that are 10.4637(11) Å apart (3-3-3) and 16.8312(19) Å apart (3-4-3). Green, light blue, gray, red, blue, and white spheres represent Mg, Zn, C, O, N, and H, respectively.



Bulky amines in the pores enhance the stability of adsorption/desorption cycles

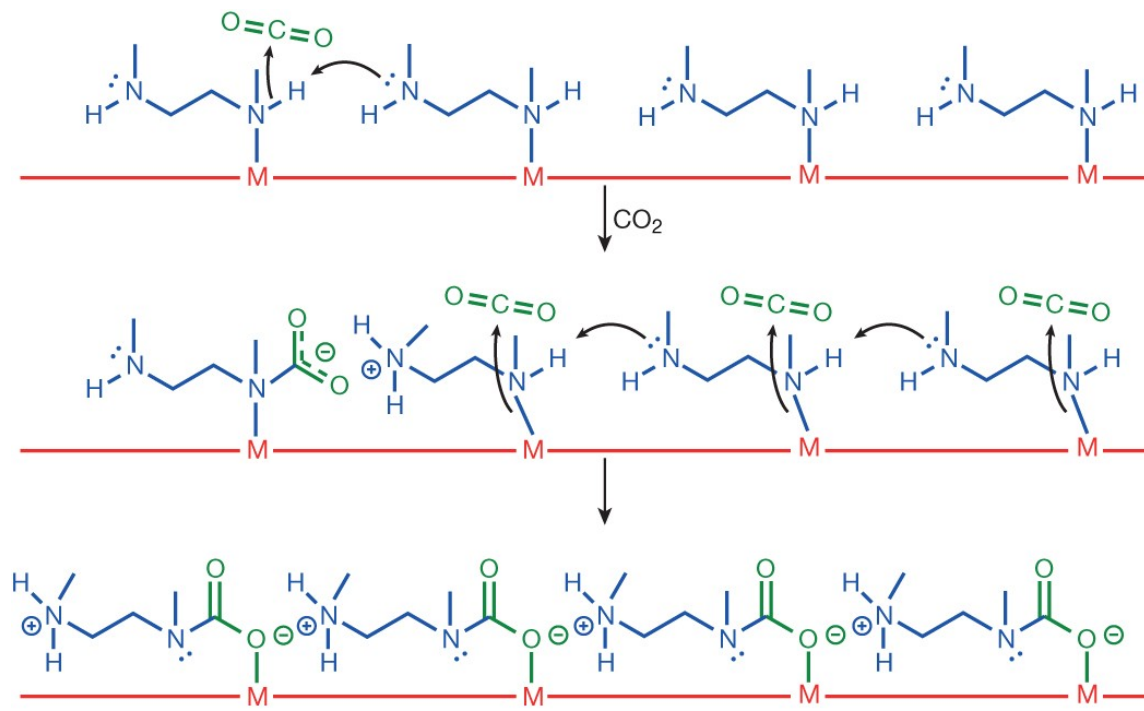
Double-step adsorption limits the capacity of MOF in  $\text{CO}_2$  capture and leads to higher regeneration temperature.

[nature](#) > [articles](#) > [article](#)

Article | Published: 11 March 2015

# Cooperative insertion of CO<sub>2</sub> in diamine-appended metal-organic frameworks

Thomas M. McDonald, Jarad A. Mason, Xueqian Kong, Eric D. Bloch, David Gygi, Alessandro Dani, Valentina Crocellà, Filippo Giordanino, Samuel O. Odoh, Walter S. Drisdell, Bess Vlaisavljevich, Allison L. Dzubak, Roberta Poloni, Sondre K. Schnell, Nora Planas, Kyuho Lee, Tod Pascal, Liwen F. Wan, David Prendergast, Jeffrey B. Neaton, Berend Smit, Jeffrey B. Kortright, Laura Gagliardi, Silvia Bordiga, ... Jeffrey R. Long 

[+ Show authors](#)

## Why this paper?

- Single-step CO<sub>2</sub> adsorption.
- Selective for CO<sub>2</sub> capture.
- This paper tells that by tuning the stearic bulk and basicity of pore-dwelling amine, CO<sub>2</sub> capture capacities can be tuned.
- ee-2-Mg(olz) captures CO<sub>2</sub> from coal flue gas.
- Basicity plays a major role in CO<sub>2</sub> capture at high temperature and low pressure.



# Introduction

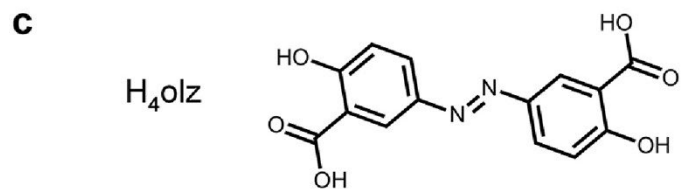
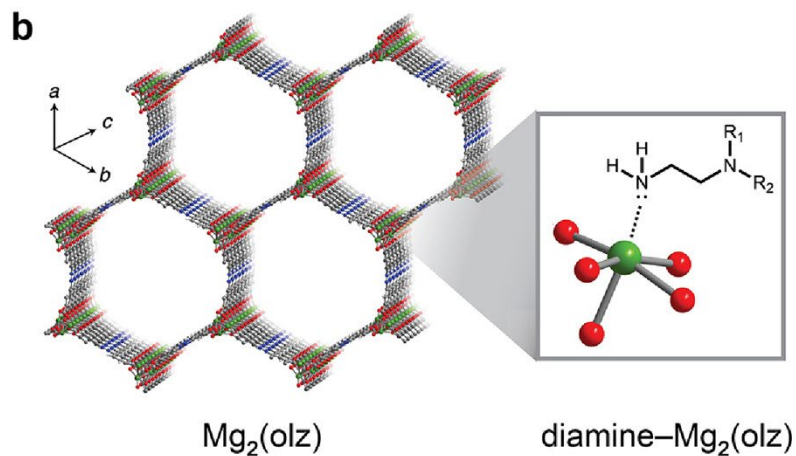
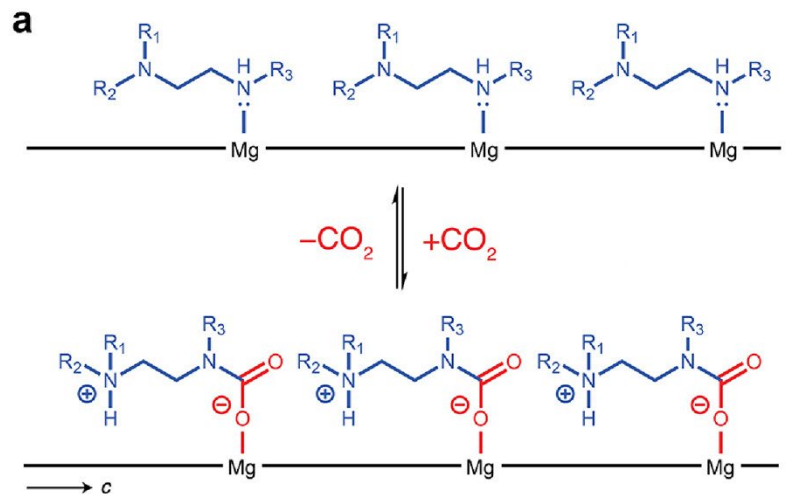


Figure 1. (a) Depiction of cooperative  $\text{CO}_2$  insertion into diamine- $\text{Mg}_2(\text{dobpdc})$  to form chains of ammonium carbamate. (b) Structure of activated  $\text{Mg}_2(\text{olz})$ , which was postsynthetically functionalized with diamines to generate diamine- $\text{Mg}_2(\text{olz})$ . Green, red, blue, gray, and white depict the Mg, N, C, and H atoms, respectively. (c) Structure of the  $\text{H}_4\text{olz}$  linker.

**Table 1. Structures and Shorthand for Diamines Used in This Work**

Diamine	Structure	Abbreviation
<i>N,N</i> -diisopropylethylenediamine		ii-2
<i>N,N</i> -dimethylethylenediamine		mm-2
<i>N,N</i> -diethylethylenediamine		ee-2
1,2-diamino-2-methylpropane		dmen
<i>N</i> -(3-pentyl)ethylenediamine		3-pent-2
<i>N</i> -isopropylethylenediamine		i-2
<i>N</i> -propylethylenediamine		p-2
<i>N</i> -ethylethylenediamine		e-2
<i>N</i> -methylethylenediamine		m-2

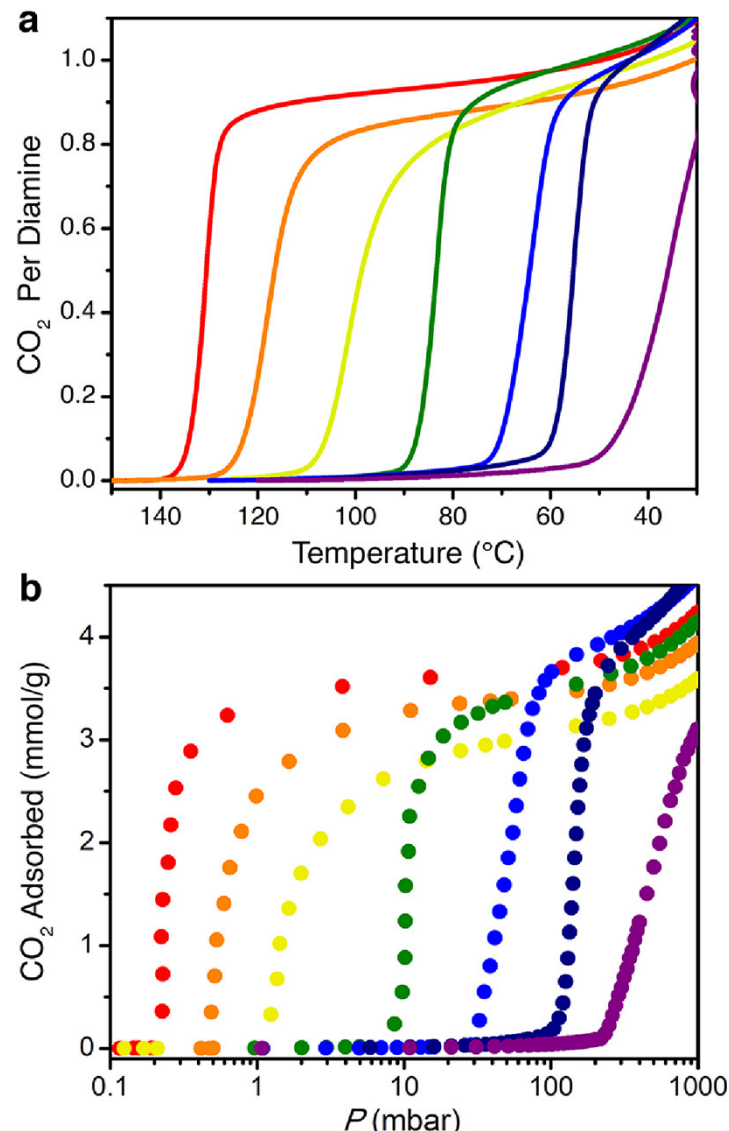


Figure 2. (a) Adsorption isobars (from left to right) obtained for e-2-, i-2-, 3-pent-2-, dmen-, ee-2-, mm-2-, and ii-2-Mg<sub>2</sub>(olz) under pure CO<sub>2</sub>, as measured by thermogravimetric analysis. (b) Pure CO<sub>2</sub> adsorption isotherms (from left to right) obtained at 40 °C for e-2-, i-2-, 3-pent-2-, dmen-, ee-2-, mm-2-, and ii-2-Mg<sub>2</sub>(olz). The data for m-2-Mg<sub>2</sub>(olz) and p-2-Mg<sub>2</sub>(olz) nearly overlay those collected for e-2-Mg<sub>2</sub>(olz) and are omitted here for simplicity. See [Figure 3a](#) for the corresponding isotherms at 85 °C for all three 1°,2°-diamines bearing linear alkyl substituents.

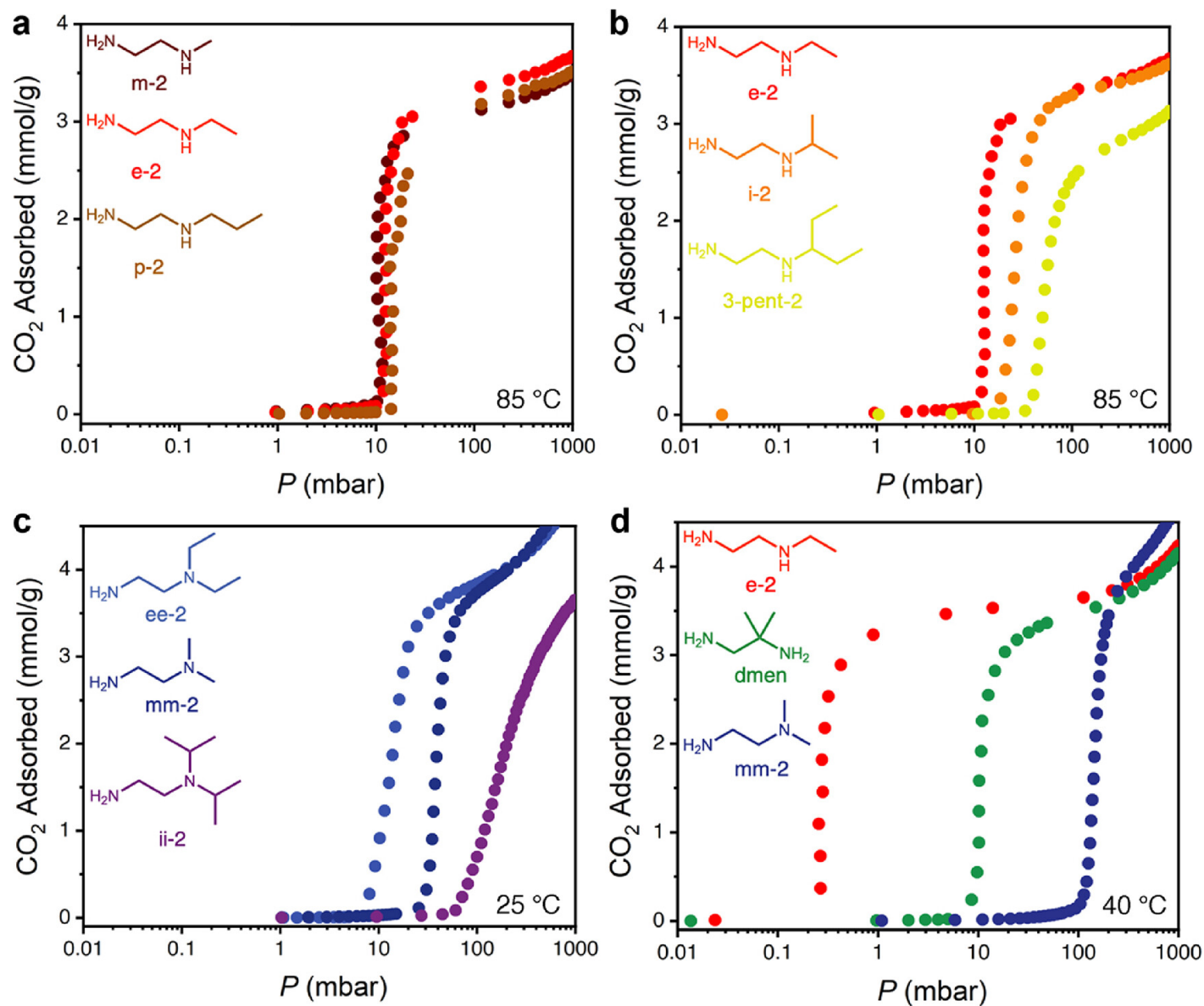


Figure 3. Comparisons of adsorption isotherms under pure  $\text{CO}_2$  for different series of diamine- $\text{Mg}_2(\text{olz})$  variants illustrating the effect of the diamine structure on the adsorption step pressure. (a) 1°,2°-Diamines bearing linear alkyl substituents, (b) 1°,2°-diamines with increasingly branched substituents, (c) 1°,3°-diamines with different degrees of substituent branching, and (d) diamines with two-carbon alkyl substitutions. Note the distinct isotherm temperatures for each series: data were collected at 85 °C for panels (a) and (b), 25 °C for panel (c), and 40 °C for panel (d).



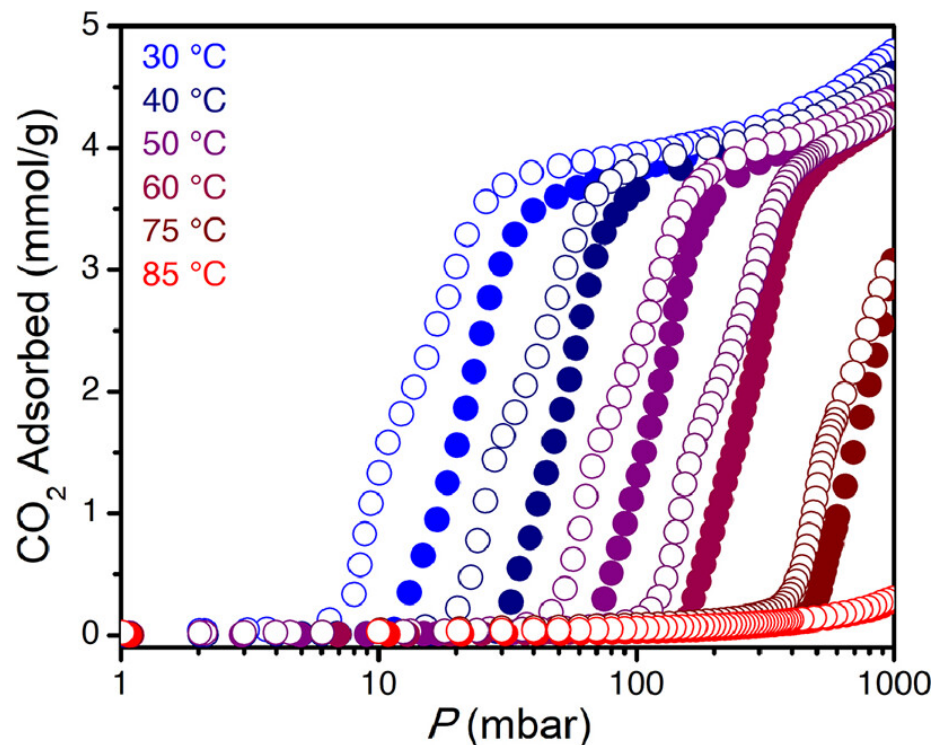


Figure 4. Carbon dioxide adsorption isotherms for ee-2-Mg<sub>2</sub>(olz) collected at the indicated temperatures with pressure plotted on a logarithmic scale. The filled and empty circles represent the adsorption and desorption data, respectively.

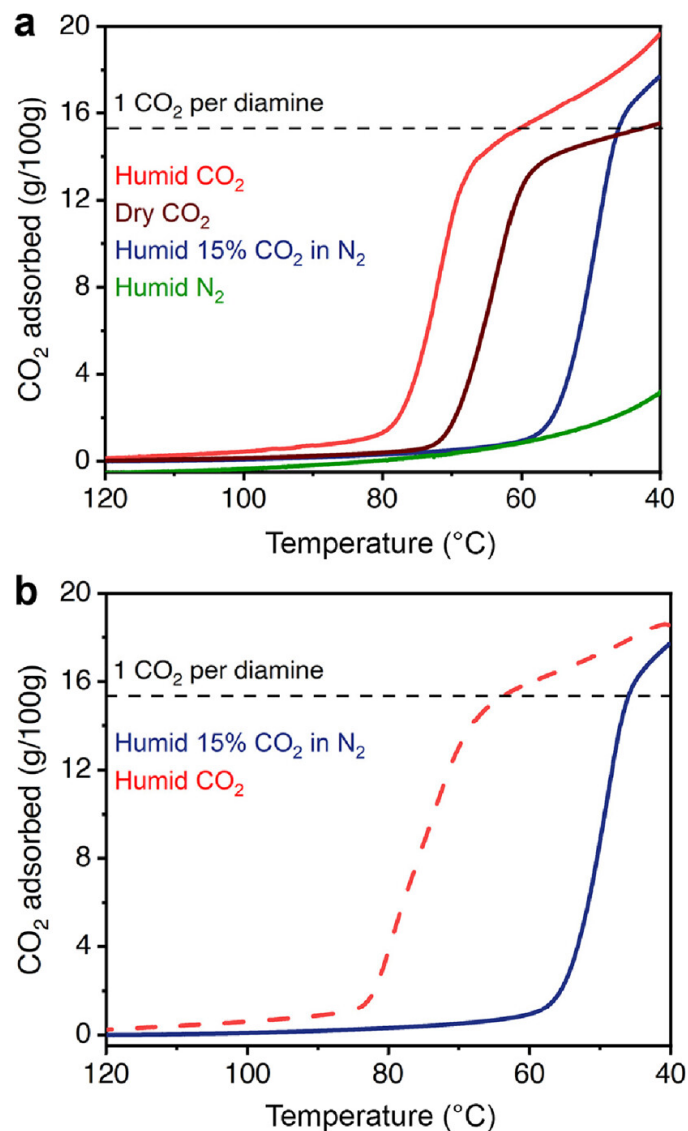


Figure 5. (a) Comparison of humid CO<sub>2</sub> (~1.5% H<sub>2</sub>O), dry CO<sub>2</sub>, humid 15% CO<sub>2</sub> in N<sub>2</sub> (~1.5% H<sub>2</sub>O), and humid N<sub>2</sub> (~1.5% H<sub>2</sub>O) adsorption isobars for ee-2-Mg<sub>2</sub>(olz) at atmospheric pressure. (b) Humid 15% CO<sub>2</sub> in N<sub>2</sub> (~1.5% H<sub>2</sub>O) adsorption isobar (cooling, solid blue line) and humid CO<sub>2</sub> (~1.5% H<sub>2</sub>O) desorption isobar (heating, dashed red line) for ee-2-Mg<sub>2</sub>(olz) under atmospheric pressure. A ramp rate of 1 °C/min was used for all of the isobaric experiments.

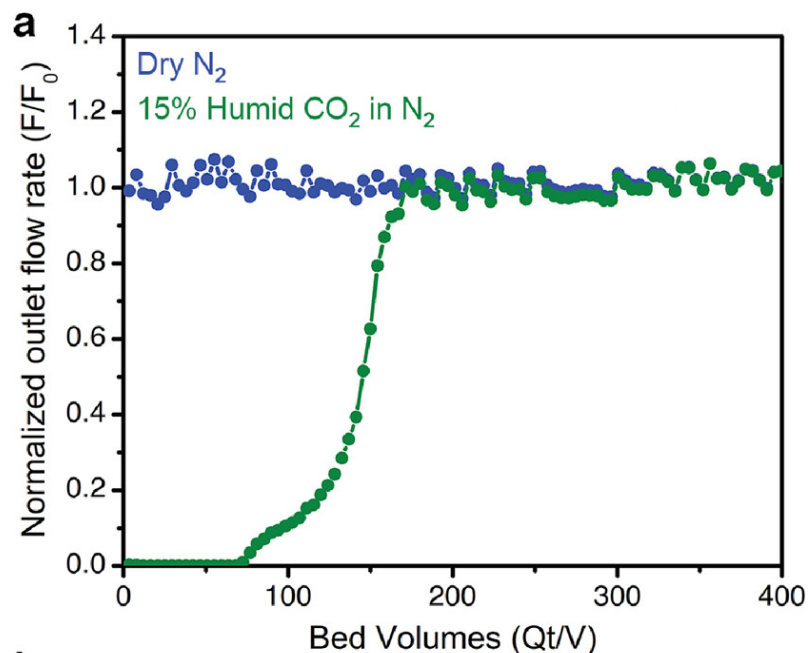
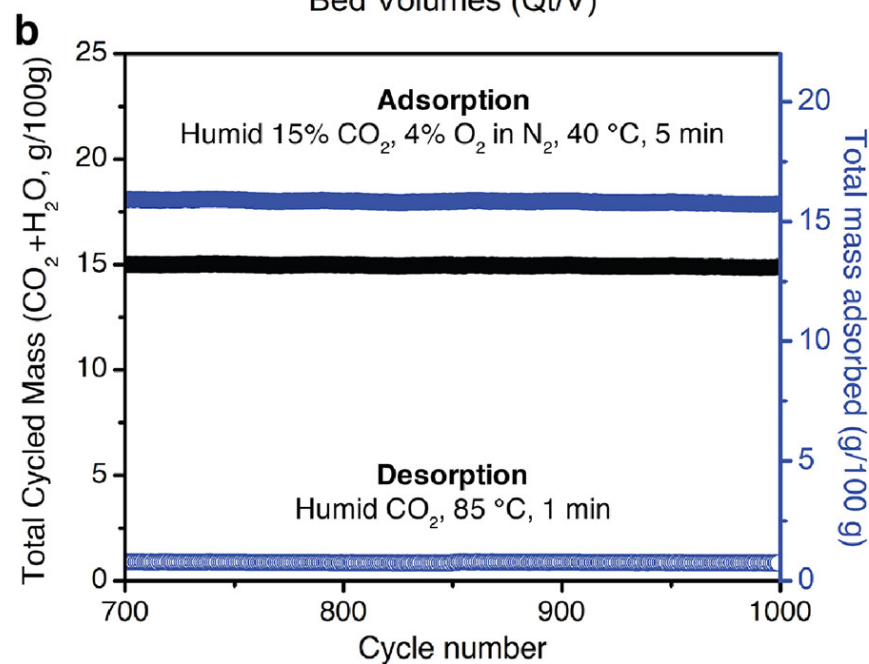


Figure 6. (a) Breakthrough data for ee-2- $Mg_2(olz)$  collected under humid ( $\sim 2.3\%$   $H_2O$ ) 15%  $CO_2$  in  $N_2$  at  $40^\circ C$  with a flow rate of 10 sccm and  $\sim 1$  bar feed pressure. Breakthrough of  $N_2$  occurred nearly immediately, indicating negligible  $N_2$  uptake. The  $CO_2$  breakthrough profile exhibits a favorable sharp shape and corresponds to a total capacity of  $3.9 \pm 0.3$  mmol/g. (b) Last 300 of 1000 thermogravimetric temperature-swing cycles conducted on ee-2- $Mg_2(olz)$  under simulated humid coal flue gas at atmospheric pressure. Adsorption,  $40^\circ C$ , humid ( $\sim 2.3\%$   $H_2O$ ) 15%  $CO_2$ , 4%  $O_2$  in  $N_2$ , 5 min; desorption,  $85^\circ C$ , humid ( $\sim 2.3\%$   $H_2O$ )  $CO_2$ , 1 min



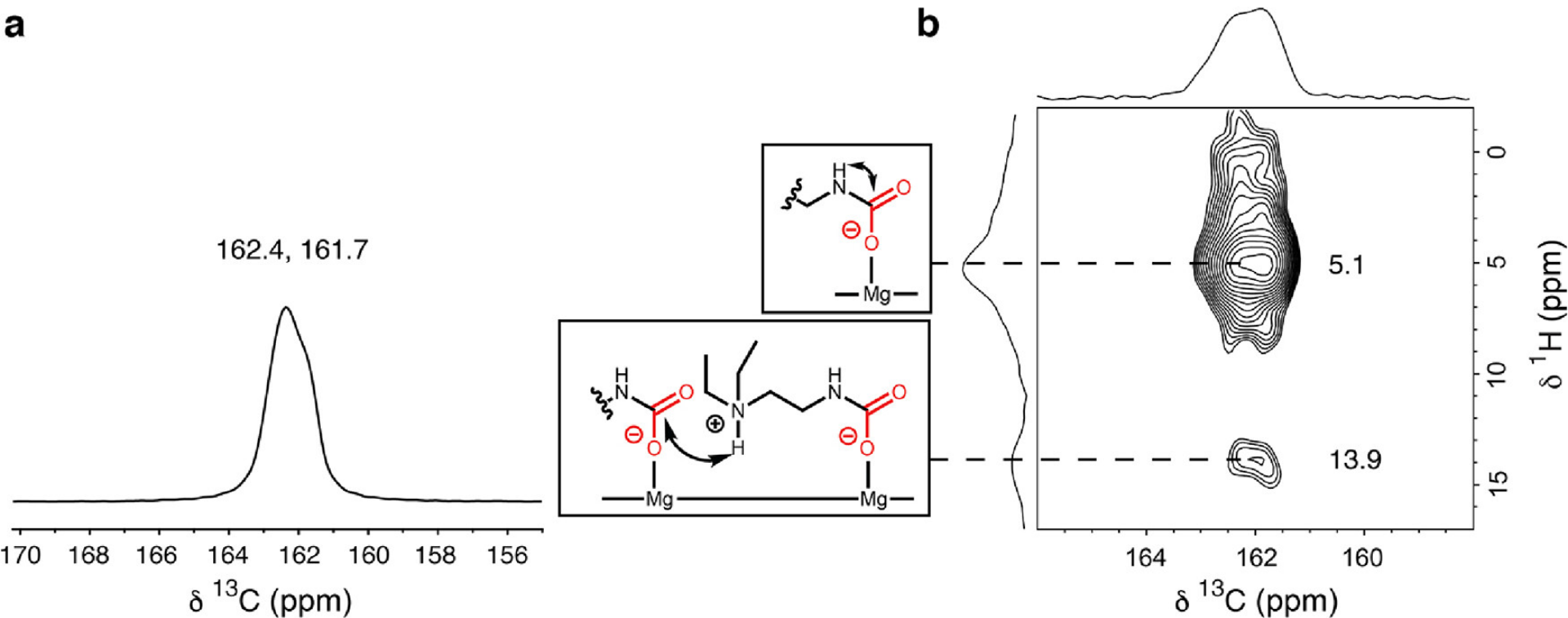


Figure 7. Room-temperature solid-state magic angle spinning NMR (16.4 T) spectra of ee-2- $\text{Mg}_2(\text{olz})$  dosed with 1 bar  $^{13}\text{CO}_2$ . (a)  $^{13}\text{C}$  NMR spectrum obtained by cross-polarization (with continuous-wave decoupling of  $^1\text{H}$ ). (b)  $^1\text{H} \rightarrow ^{13}\text{C}$  HETCOR (contact time 100  $\mu\text{s}$ ) spectrum and correlation assignments.

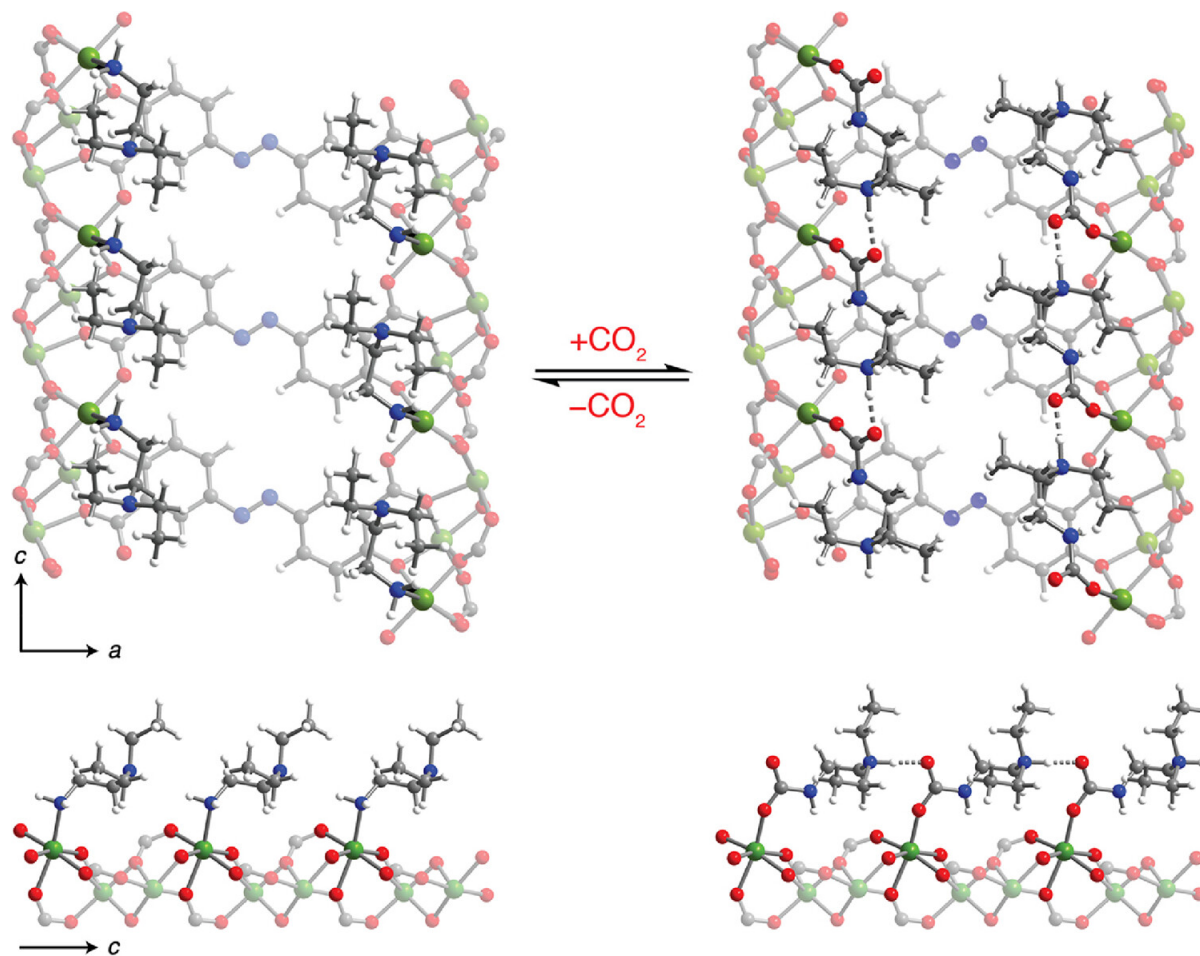


Figure 8. Proposed structures of (left) evacuated  $ee-2-Mg_2(olz)$  and (right) ammonium carbamate chains formed upon the adsorption of  $CO_2$  in  $ee-2-Mg_2(olz)$ . Green, red, blue, gray, and white spheres represent Mg, O, N, C, and H, respectively.

Theoretical BE- -66.4 Kj/mol  
 Experimental BE- -69.9 Kj/mol

## Conclusion

A class of MOFs has been developed where small temperature swings can be used to capture CO<sub>2</sub>.

Both the steric factor and the basicity of the pore-dwelling amine are important factors to consider in tuning the CO<sub>2</sub> adsorption step pressure or temperature.

Amine steric bulk is inversely proportional to the degree of CO<sub>2</sub> cooperativity.

MOF was thermally and oxidatively stable